MECHANISMS OF SIGNAL TRANSDUCTION:

Evidence for a Model of Agonist-induced Activation of 5-Hydroxytryptamine 2A Serotonin Receptors That Involves the Disruption of a Strong Ionic Interaction between Helices 3 and 6 ,

David A. Shapiro, Kurt Kristiansen, David M. Weiner, Wesley K. Kroeze and Bryan L. Roth

J. Biol. Chem. 2002, 277:11441-11449.
doi: 10.1074/jbc.M111675200 originally published online January 18, 2002

THE JOURNAL OF BIOLOGICAL CHEMISTRY
Vol. 277, No. 13, Issue of March 29, pp. 11441–11449, 2002
Printed in U.S.A.

Evidence for a Model of Agonist-induced Activation of 5-Hydroxytryptamine 2A Serotonin Receptors That Involves the Disruption of a Strong Ionic Interaction between Helices 3 and 6*[S]

Received for publication, December 7, 2002
Published, JBC Papers in Press, January 18, 2002, DOI 10.1074/jbc.M111675200

David A. Shapiro‡, Kurt Kristiansen§, David M. Weiner¶, Wesley K. Kroeze‡, and Bryan L. Roth‡‖

From the ‡Department of Biochemistry, Case Western Reserve University Medical School, Cleveland, Ohio 44106-4935, ¶ACADIA Pharmaceuticals, Inc., San Diego, California 92121 and the Departments of Neurosciences and Psychiatry, University of California at San Diego, La Jolla, California, and the §Department of Pharmacology, Institute of Pharmacy, University of Tromsø, Tromsø N-9037, Norway

5-Hydroxytryptamine 2A (5-HT2A) receptors are essential for the actions of serotonin (5-hydroxytryptamine (5-HT)) on physiological processes as diverse as vascular smooth muscle contraction, platelet aggregation, perception, and emotion. In this study, we investigated the molecular mechanism(s) by which 5-HT activates 5-HT2A receptors using a combination of approaches including site-directed mutagenesis, molecular modeling, and pharmacological analysis using the sensitive, cell-based functional assay R-SAT. Alanine-scanning mutagenesis of residues close to the intracellular end of H6 of the 5-HT2A receptor implicated glutamate Glu-318(6.30) in receptor activation, as also predicted by a newly constructed molecular model of the 5-HT2A receptor, which was based on the x-ray structure of bovine rhodopsin. Close examination of the molecular model suggested that Glu-318(6.30) could form a strong ionic interaction with Arg-173(3.50) of the highly conserved "(D/E)RY motif" located at the interface between the third transmembrane segment and the second intracellular loop (i2). A direct prediction of this hypothesis, that disrupting this ionic interaction by an E318(6.30)R mutation would lead to a highly constitutively active receptor with enhanced affinity for agonist, was confirmed using R-SAT. Taken together, these results predict that the disruption of a strong ionic interaction between transmembrane helices 3 and 6 of 5-HT2A receptors is essential for agonist-induced receptor activation and, as recently predicted by ourselves (B. L. Roth and D. A. Shapiro (2001) *Expert Opin. Ther. Targets* 5, 685–695) and others, that this may represent a general mechanism of activation for many, but not all, G-protein-coupled receptors.

5-Hydroxytryptamine 2A (5-HT2A)[1] receptors are essential for the actions of serotonin (5-hydroxytryptamine; 5-HT) on a number of key physiological processes including platelet aggregation, vascular and nonvascular smooth muscle contraction, perception, and emotion (1). Additionally, 5-HT2A receptors represent a major site of action of hallucinogens such as lysergic acid diethylamide, which are agonists, and atypical antipsychotic drugs such as clozapine, which are antagonists (2). 5-HT2A receptors are unique in that both agonists and antagonists induce receptor internalization (3) that is dynamin-dependent and arrestin-independent (4). Despite considerable study (5–9), the molecular and atomic mechanisms by which 5-HT induces activation of the 5-HT2A receptor or of the other 15 cloned 5-HT receptors are currently unknown.

Prior studies have suggested several potential models of agonist-induced activation of 5-HT receptors in particular and other G-protein-coupled receptors (GPCRs) in general. Initial site-directed mutagenesis studies of the 5-HT2A (10) and α_{1b}-adrenergic receptors (11, 12) as well as rhodopsin (13) implicated a negatively charged residue in transmembrane helix 3 (H3), which could form a strong interaction with positively charged/polar residues in H7 ("H3-H7 interaction model"). Another model ("H2-H7 proximity model") (7) suggested that hydrogen bonding interactions between H2 and H7 were most important for the activation of 5-HT2A receptors and gonadotrophic hormone receptors (14). Predictions based on the H2-H7 proximity model suggest that this could be a general model for GPCR activation (14, 15). More recent studies have predicted that agonist-induced activation of rhodopsin and β_2-adrenergic receptors (16, 17) and muscarinic m5 receptors (18, 19) occurs via agonist-induced rotations of H6 and H3 ("H3-H6 rotation model"). This model was quite recently modified based on examination of the crystal structure of rhodopsin (20) and extended to include disruption of a strong ionic interaction between residues in H6 and H3 ("H6-H3 interaction model") (21, 41). Indeed, the H6-H3 interaction model has recently been supported by mutagenesis and modeling studies of the β_2-adrenergic receptor (21).

In recent studies (6, 9), we demonstrated that the H3-H7 interaction model does not adequately describe agonist-induced 5-HT2A receptor activation. Instead, we have proposed (6, 22) that agonists interact with H6 via aromatic residues and that this interaction facilitates H6 motion and subsequent receptor activation. We have also predicted (41) that agonist binding to

* This work was supported in part by Grants RO1MH57635 (to B. L. R.) and KO2MH01366 (to B. L. R.), from the National Institutes of Health and a NARSAD Young Investigator Award (to D. S.). The costs of publication of this article were defrayed in part by the payment of page charges. This article must therefore be hereby marked "*advertisement*" in accordance with 18 U.S.C. Section 1734 solely to indicate this fact.

[S] The on-line version of this article (available at http://www.jbc.org) contains the molecular dynamics trajectories (500–1000 ps) of the WT 5-HT2A receptor, V328A, E318R, and the E318R/R173E double mutants. To view these supplemental materials, you will require a program capable of viewing AMBER crd and parm files. One such program, VMD for Microsoft Windows, Apple Macintosh, and UNIX is available on the World Wide Web at http://www.ks.uiuc.edu/Research/vmd/ (developed by the Theoretical Biophysics Group at the University of Illinois).

‖ To whom correspondence should be addressed: Dept. of Biochemistry, W438 Case Western Reserve University Medical School, 10900 Euclid Ave., Cleveland, OH 44106-4935. Tel.: 216-368-2730; Fax: 216-368-3419; E-mail: roth@biocserver.cwru.edu.

[1] The abbreviations used are: 5-HT2A, 5-hydroxytryptamine 2A; 5-HT, 5-hydroxytryptamine; TM, transmembrane; PI, phosphoinositide; GPCR, G-protein-coupled receptor; WT, wild type; DOI, 2,5-dimethoxy-4-iodophenyl-2-aminopropane.

residues in H6 leads to the disruption of a strong ionic interaction between H3 and H6. In the current study, we test this "H3-H6 interaction model" via a combination of site-directed mutagenesis and molecular modeling studies. Functional expression via R-SAT (receptor selection and amplification technology) was used to characterize the effects of receptor mutations on basal, agonist-independent receptor activity. Taken together, these results are consistent with a model of 5-HT2A receptor activation in which agonists induce a disruption of a strong ionic interaction between H3 and H6, which is facilitated by agonist-induced movements of H6. We also suggest, based on an examination of aligned amino acids, that this is likely to be a widely used, although not universal, mechanism for agonist-mediated activation of G-protein coupled 5-HT receptors.

MATERIALS AND METHODS

Receptor Numbering Schemes—Where appropriate, amino acid residues have been labeled both by standard amino terminus-based numbering and parenthetically by a numbering scheme introduced in 1995 by Ballesteros and Weinstein (23) in which relative amino acid positions are highlighted. This scheme facilitates the efficient comparison of residues within different GPCRs. With this method, every amino acid identifier starts with the transmembrane helix number and is followed by the position relative to a reference residue (arbitrarily assigned the number 50) among the most conserved amino acids in that transmembrane helix. In the seven-transmembrane (TM) GPCRs, this generalized numbering scheme utilizes Asn-1.50, Asp-2.50, Arg-3.50, Trp-4.50, Pro-5.50, Pro-6.50, and Pro-7.50 as seven reference positions, corresponding in rat 5-HT2A receptors to Asn-92, Asp-120, Arg-173, Trp-200, Pro-246, Pro-338, and Pro-377, respectively. Phe-340, for example, lies two positions positive relative to Pro-338, yielding the identifier (6.52), while one of the key residues studied in this manuscript, Arg-173(3.50) is itself the most highly conserved residue in TM3.

Constructs and Antibodies—Mutant rat 5-HT2A receptors, expressed in either pSVK3 (Amersham Biosciences, Inc.) or pCDNA3.1 (Invitrogen, Carlsbad, CA) were constructed by a PCR-based mutagenesis technique as previously detailed for use in radioligand binding, phosphoinositide (PI) hydrolysis, and confocal microscopic studies (4, 6). A 5-HT2A-specific antibody was used for fluorescent confocal microscopic studies as recently described (4). For R-SAT studies, mutations of 5-HT2A receptors were performed as previously detailed (24). All mutations were confirmed by automated, fluorescent sequencing of the entire insert (Cleveland Genomics, Cleveland, OH).

Transfection and Expression of Mutant 5-HT2A Receptors for Radioligand Binding and PI Hydrolysis Experiments—Transfections of HEK-293 cells were performed using Fugene-6 as previously described (4, 6). For radioligand binding assays, cells were switched 24 h after transfection to Dulbecco's modified Eagle's medium containing 5% dialyzed fetal calf serum, and 24 h later they were switched to serum-free Dulbecco's modified Eagle's medium. Cells were then harvested 24 h later for radioligand binding assays, which were performed as previously described (4, 6). PI hydrolysis experiments were performed exactly as previously detailed (4, 6). Receptor expression was verified concurrently with binding experiments by immunohistochemistry using an antibody specific for the 2A receptor.

R-SAT Assays—R-SAT (ACADIA Pharmaceuticals, San Diego, CA) assays were performed with minor modifications from those previously described (18, 19, 25). Briefly, NIH-3T3 cells were grown in 96-well tissue culture plates to 70–80% confluence in Dulbecco's modified Eagle's medium supplemented with 10% calf serum and 1% penicillin/streptomycin/Gln. Cells were transfected for 12–16 h with plasmid DNAs using Superfect Reagent (Qiagen, Valencia, CA) per the manufacturer's protocols. R-SATs were performed with 0.5–50 ng/well receptor and 20 ng/well β-galactosidase plasmid DNA. After overnight transfection, medium was replaced with serum-free Dulbecco's modified Eagle's medium containing 2% cyto-sf3 (Kemp Biotechnologies, Frederick, MD) and 1% penicillin/streptomycin/Gln and varying concentrations of drug. Cells were grown in a humidified atmosphere with 5% ambient CO_2 for 4–6 days. Medium was removed from the plates, and β-galactosidase activity was measured by the addition of *o*-nitrophenyl β-D-galactopyranoside (in phosphate-buffered saline with 5% Nonidet P-40 detergent). The resulting colorimetric reaction was measured in a spectrophotometric plate reader (Titertek, Huntsville, AL) at 420 nM. All data were analyzed using the computer programs Excel Fit and Prism (GraphPad, San Diego, CA). Significant differences were determined by Student's *t* test.

Molecular Modeling of Wild Type and Mutant 5-HT2A Receptors—Energy minimizations and molecular dynamics simulations were performed using the all atomic force field of the AMBER (Assisted Model Building with Energy Refinement) 5.0 programs (26). Models of wild type and mutant receptors were refined by using 500 steps of steepest descent minimization followed by conjugate gradient energy minimization until convergence with a 0.005 kcal mol^{-1} $Å^{-1}$ root mean square energy gradient difference between successive minimization steps. A distance-dependent dielectric function ($e = r_{ij}$) and a 10-Å cut-off radius for nonbonded interactions were used.

Molecular dynamics simulations *in vacuo* were performed for 1 ns at 300 K. The temperature was increased to 300 K during the first 30 ps of each simulation. This was followed by an equilibrium period (30–500 ps) and a production run (500–1000 ps). For analysis purposes, structures were collected every 1 ps. The bond lengths involving hydrogens were constrained by using the SHAKE algorithm, allowing an integration step of 0.001 ps. The secondary structure of helices was preserved using distance restraints. These restraints were applied between the backbone oxygen atom of residue i and the HN hydrogen atom of residue $i + 4$ in H1–H7 and the cytoplasmic helix, excluding prolines and the part of H7 that attain a 3/10 helical conformation (restraints between the backbone oxygen atom of residue i and the HN hydrogen atom of residue $i + 3$). The ICM (Internal Coordinate Mechanics) 2.8 Pro program (Molsoft L.L.C., La Jolla, CA) was used for all computer graphics visualizations, for Biased Probability Monte Carlo simulations (27), and for calculation of accessible surface area.

A model of the rat $5\text{-}HT_{2A}$ receptor was constructed by using computer graphics and molecular mechanics energy calculations. The model included all parts of the amino acid sequence (residue ranges as follows: Leu-71(1.29)–Thr-266(5.70) and Met-312(6.24)–Gln-398(7.71)) with the exception of the amino-terminal segment and most of the carboxyl-terminal and third intracellular loop segments.

An initial model comprising the seven transmembrane helices, the short loop between H1 and H2, a putative cytoplasmic helix after H7, and part of the second extracellular loop was built by using the x-ray structure of the inactive state conformation of bovine rhodopsin (20) as a template. By using the WHATIF program (28), amino acid residues in these parts of the bovine rhodopsin structure (chain A) were substituted to their rat $5HT_{2A}$ receptor counterparts. According to the mutation data in Ref. 6, the rotational orientation of helix 5 was modified such that the Phe-340(5.44) side chain pointed away from the binding site and the Phe-243(5.47) and Phe-5.48 side chains pointed into the binding site. The loop search feature of the SWISS-PDB VIEWER (version 3.7 beta 2) program (29) was used to identify candidate conformations for each of the loops.

The extreme N- and C-terminal parts of the long third intracellular loop were built as ideal α-helical extensions of H5 and H6 using the SWISS-PDB VIEWER. The C terminus of helices at Thr-266(5.70) and Gln-398(7.71) was capped by NCH_3, whereas the N terminus of helices at Leu-71(1.29) and Met-312(5.24) was capped by $COCH_3$. Model 1 was obtained by energy minimization of this model. Two disulfide bridges, Cys-148(3.25)-Cys-227 (second extracellular loop) and Cys-349–Cys-353 (within the third extracellular loop), were introduced during the energy minimization.

Models of the R173(3.50)E/E318(6.30)R, E318(6.30)R, and V328(6.40)A mutants were constructed by substituting amino acids in model 1 of the wild type receptor using ICM. The side chain dihedral angles of residues at or near positions 3.50 and 6.30 in the R173(3.50)E/E318(6.30)R, E318(6.30)R mutants were optimized by 100,000 steps in biased probability Monte Carlo simulations (27) using the ECEPP/3 force field in ICM. The Monte Carlo stack conformation having the lowest potential energy was further refined by energy minimization using AMBER. The resultant energy-minimized models and model 1 of the wild type receptor were used as the starting structure for molecular dynamics simulations. An average conformation was calculated over the last 500 ps of each molecular dynamics trajectory by using the CARNAL program. This conformation was subsequently energy-minimized using AMBER. The resulting models have been designated model 2 of the wild type and mutant receptors.

RESULTS

Alanine-scanning Mutagenesis Identifies Residues in H6 That Alter Agonist-induced 5-HT2A Receptor Activation—In initial studies, we performed alanine-scanning mutagenesis of 12 residues (Ser-316(6.28)–Val-328(6.40)) at the *i*3/H6 inter-

TABLE I
Binding properties of WT 5-HT2A receptors and mutants

Saturation experiments using [^{125}I]-DOI and competition binding studies using [^{3}H]ketanserin were performed on membrane preparations from HEK 293 cells transiently expressing WT or mutant receptors. Values represent the means of three or more experiments ± S.E. All calculations were obtained using the software program Ligand for DOS.

Mutant	K_d DOI	B_{max}	K_i 5-HT
	nM	*fmol/mg*	*μM*
WT 2A	0.47 ± 0.09	173 ± 14	0.90 ± 0.17
S316A	0.46 ± 0.05	412 ± 21	1.2 ± 0.06
N317A	0.43 ± 0.07	357 ± 21	2.1 ± 0.59[a]
E318A	0.26 ± 0.08	1137 ± 136	0.29 ± 0.05[a]
Q319A	0.67 ± 0.10	491 ± 34	1.1 ± 0.49
K320A	3.17 ± 0.89[a]	108 ± 10	1.5 ± 0.32
C322A	0.87 ± 0.14	285 ± 20	0.38 ± 0.11[a]
K323A	0.74 ± 0.18	180 ± 16	0.54 ± 0.17
V324A	0.89 ± 0.17	306 ± 24	0.25 ± 0.10[a]
L325A	0.90 ± 0.09	324 ± 9.7	0.10 ± 0.01[a]
G326A	0.52 ± 0.08	272 ± 16	0.29 ± 0.07[a]
I327A	0.62 ± 0.10	219 ± 15	0.26 ± 0.13[a]
V328A	0.28 ± 0.02	728 ± 36	0.62 ± 0.37

[a] Significantly different from WT ($p \leq 0.05$).

face. The residues at positions 6.33–6.37 are assumed to be localized at a mixed hydrophobic-hydrophilic environment at the lipid/water interface as proposed from spin labeling experiments with rhodopsin (30). As shown in Table I, all of these mutant receptors were expressed as functional receptors as measured by [^{125}I]DOI binding, although some variations in receptor expression were measured. Immunochemical studies also verified receptor expression (not shown). Table I also shows that all mutants retained low micromolar or submicromolar affinities for 5-HT, although most mutants had slightly increased (E318(6.30)A, C322(6.34)A, V324(6.36)A, L325(6.37)A, G326(6.38)A, and I327(6.39)A) or decreased (N317(6.29)A) affinities for 5-HT. Taken together, these results imply that none of the residues is directly involved in ligand binding, since very little change in [^{125}I]DOI binding affinity was detected and that the effects on agonist binding are likely to be allosteric in nature.

We next examined the ability of these 12 H6 mutants to be activated by 5-HT via measurements of 5-HT-mediated PI hydrolysis. As shown in Fig. 1 and Table II, the various mutant 5-HT receptors were differentially affected by alanine mutagenesis. Four classes of mutations were discovered: 1) mutations that enhanced the potency of 5-HT-stimulated PI hydrolysis (E318(6.30)A, C322(6.34)A, V324(6.36)A, V328(6.40)A); 2) mutations that diminished the potency of 5-HT-stimulated PI hydrolysis (N317(6.29)A, Q319(6.31)A, K320(6.32)A); 3) mutations that reduced the efficacy of 5-HT-stimulated PI hydrolysis (L325(6.37)A); and 4) mutations that had no effect on 5-HT-stimulated PI hydrolysis (S316(6.28)A, K323(6.35)A, G326(6.38)A, I327(6.39)A). Visualization of the locations of these residues in a 5-HT2A receptor model (model 1, Fig. 2*a*) suggests that where mutation to alanine enhances agonist potency, it probably does so via distinct mechanisms. Among these, Glu-318(6.30) appeared to form an ionic interhelical interaction with Arg-173(3.50), whereas the hydrophobic residues had their side chains directed toward hydrophobic residues in H5 (Cys-322(6.34)) or H7 (Val-324(6.36), Val-328(6.40)).

The side chains of all residues where mutation to alanine decreased potency are predicted to be involved in intrahelical hydrogen bonding interactions in model 1 (Fig. 2*b*, pre-MD simulation). The side chain CO moiety of Gln-319(6.31) interacted with the NH_3^+ moiety of Lys-320(6.32), whereas the NH_2 moiety of Asn-317(6.29) interacted with one carboxylate oxygen

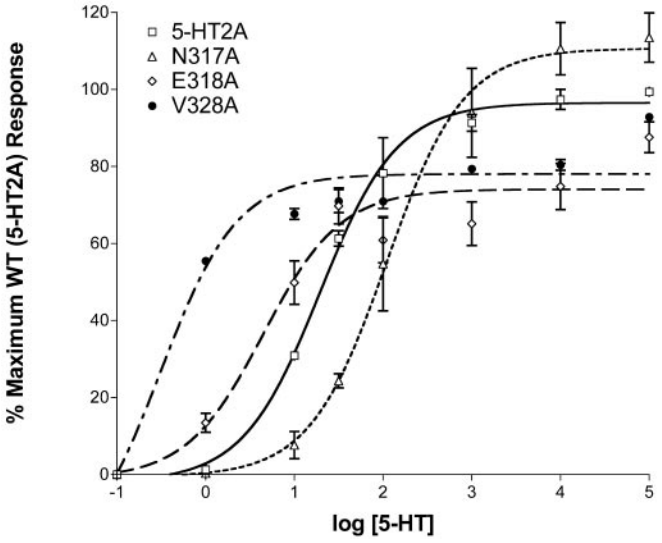

FIG. 1. **Representative agonist-mediated PI hydrolysis Isotherms.** Data represent means ± S.E. of triplicate determinations for the percentages of stimulation of PI hydrolysis in cells transfected with wild type 5-HT2A or mutant receptors. Six log-serial dilutions of 5-HT were incubated in a 24-well tissue culture plate in wells containing transiently transfected HEK 293 cells, and the accumulation of [^{3}H]-inositol monophosphate was determined as described under "Materials and Methods." Data are expressed as percentages of native receptor stimulation and are representative of three separate experiments.

TABLE II
WT and mutant receptor activation by 5-HT

PI hydrolysis activation isotherms for serotonin were obtained from HEK 293 cells transiently transfected with WT or mutant receptors as described. K_{act} values were calculated from EC_{50} using the software program GraphPad Prism. Values represent the means of three or more experiments ± S.E.

Mutant	K_{act}	V_{max}
	nM	*%WT*
WT 2A	18.1 ± 1.2	101.2 ± 4.1
S316A	36.8 ± 9.0	92.0 ± 5.1
N317A	91.5 ± 20.6[a]	91.6 ± 13.0
E318A	4.0 ± 1.5[a]	88.5 ± 14.1
Q319A	47.0 ± 17.2[a]	71.3 ± 6.7
K320A	137.4 ± 17.5[a]	67.8 ± 9.5
C322A	7.9 ± 0.20[a]	87.0 ± 3.6
K323A	10.4 ± 2.4	70.2 ± 16.6
V324A	6.7 ± 1.2[a]	94.3 ± 19.3
L325A	39.0 ± 4.3	31.3 ± 8.2[a]
G326A	7.7 ± 1.7	90.1 ± 11.4
I327A	22.6 ± 5.1	77.1 ± 6.8
V328A	0.54 ± 0.04[a]	92.3 ± 11.1

[a] Significantly different from WT ($p \leq 0.05$).

atom of Glu-318(6.30). In model 2 of the wild type receptor, the Asn-317(6.29) side chain interacted with residues at the junction between H7 and the cytoplasmic helix (OH moiety of Thr-386 (7.59) and main chain NH moiety of Lys-385 (7.58)), whereas the Lys-320(6.32) side chain interacted with residues in H5 (main chain CO moiety of Ala-265 (5.69)) and the side CO moiety of Gln-319(6.31).

All residues where mutation to alanine did not affect 5-HT-stimulated receptor activation (Ser-316(6.28), Lys-323(6.35), Ile-327(6.39)) were localized on the membrane-facing surface of H6 (Fig. 2*b*). The side chain of Leu-325(6.37), where mutation to alanine decreased efficacy of 5-HT-stimulated PI hydrolysis, was predicted to be localized in the cavity formed between the transmembrane helices 2, 3, 6, and 7.

Molecular Modeling Predicts a Strong Ionic Interaction between H3 and H6 of the 5-HT2A Receptor—The localizations in model 1 of the various residues of the 5-HT2A receptor that

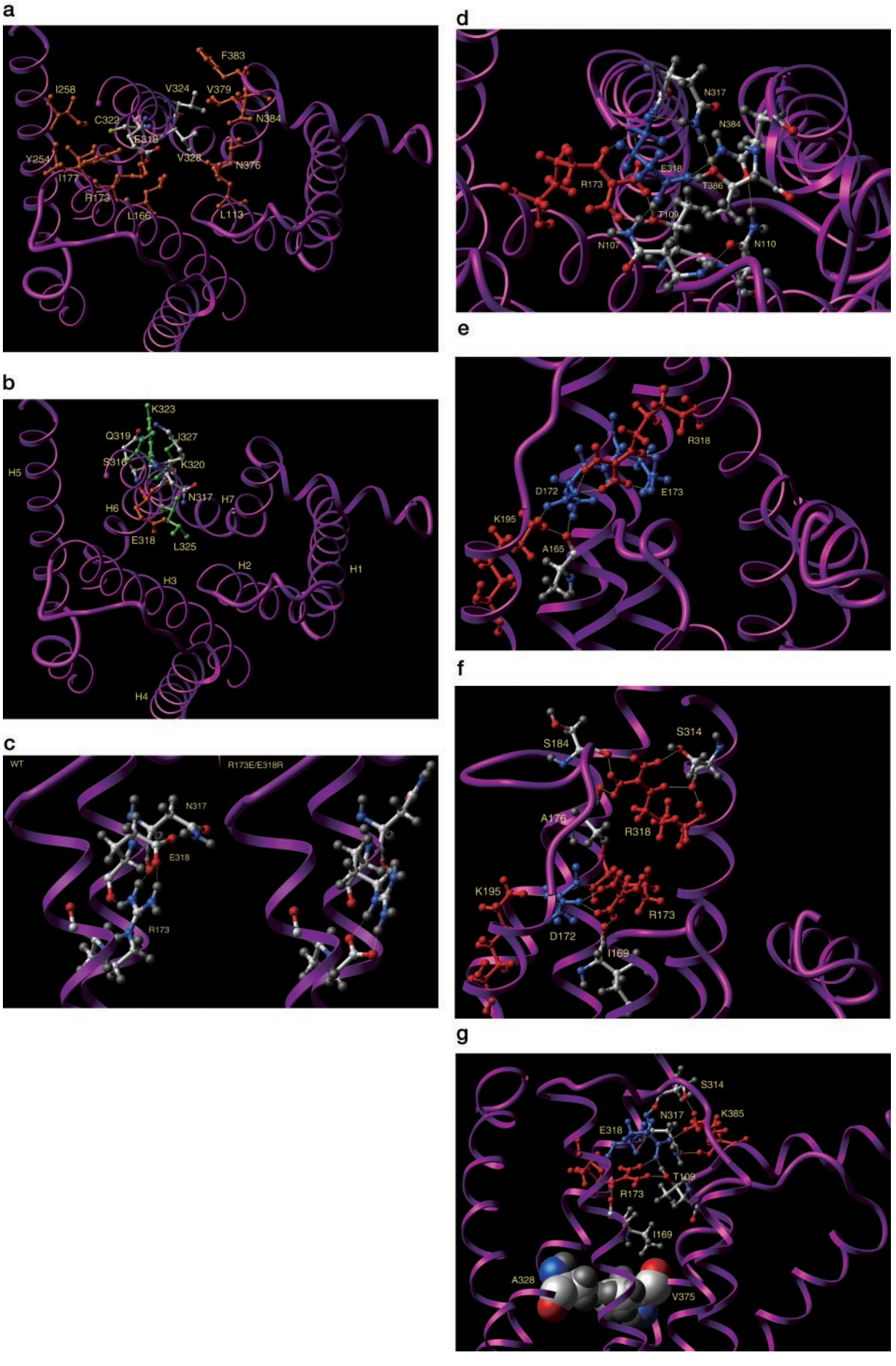

TABLE III
Binding and activation properties for WT2A and the reciprocal mutants

Binding studies using [^{3}H]ketanserin and activation data were collected as described. Values represent the means of three or more experiments ± S.E.

Mutant	K_d Ketanserin	B_{max}	K_i 5-HT	EC_{50} 5-HT
	nM	*fmol/mg*	*nM*	*nM*
5-HT2A	0.53 ± 0.14	1381 ± 994	419.8 ± 116.1	29.0 ± 6.0
R173E	0.26 ± 0.09	208 ± 160	473.6 ± 156.3	936 ± 134[a]
E318R	0.54 ± 0.11	737 ± 442	49.4 ± 11.2[a]	1.25 ± 0.36[a]
R173E/E318R	0.36 ± 0.08	618 ± 396	464.3 ± 168.3	358 ± 121[a]

[a] Significantly different from WT ($p \leq 0.05$).

were targeted for alanine-scanning mutagenesis are shown in Fig. 2, *a* and *b*. In this model, the carboxylate moiety of Glu-318(6.30) was involved in 1) salt bridge/hydrogen bonding interactions with the two NH_2 moieties of Arg-173(3.50) and 2) a hydrogen bonding interaction with the NH_2 of Asn-317(6.29), respectively (Fig. 2*c*). In model 2, the interaction between Arg-173(3.50) and Glu-318(6.30) side chains was purely electrostatic and did not involve any direct hydrogen bonding interactions (Fig. 2*d*). During the molecular dynamics simulation, the side chains of Arg-173(3.50) and Glu-318(6.30) took part in a network of hydrogen bonding interactions involving polar side chains in H2, H6, and H7. The OH moiety of Thr-109(2.39) interacted with the COO^- moiety of Glu-318(6.30) and the side chain of Arg-173(3.50) as a hydrogen bond donor and acceptor, respectively. In addition, the side chain of Arg-173(3.50) interacted through hydrogen bonding interactions with the backbone CO group of Glu-318(6.30), whereas the COO^- moiety of Glu-318(6.30) interacted through hydrogen bonding interactions with the NH_2 moiety of Asn-107(2.37), the OH moiety of Thr-386(7.59), and the NH_2 moiety of Asn-384(7.57).

Molecular Modeling of Wild Type and Mutant 5-HT2A Receptors Reveals Differences in Hydrogen Bonding Interactions—Comparison of models 1 of wild type and the R173(3.50)E/E318(6.30)R double mutant receptors revealed that the arginine side chain adopted different conformations at positions 3.50 and 6.30 (Fig. 2*c*). In the wild type receptor, the R173(3.50) side chain adopted a conformation that allows both of its NH_2 moieties to form hydrogen bonds to the carboxylate moiety of Glu-318(6.30). In contrast, the Arg-318(6.30) side chain adopted a conformation that allows its NH/NH_2 face to interact with E173(3.50) in the double mutant. This hydrogen bonding/salt bridge interaction was also present in model 2 of the R173(3.50)E/E318(6.30)R double mutant (Fig. 2*e*). However, additional interactions between the NH_2/NH_2 face of R318 and the carboxylate moiety of D172(3.49) were also observed in model 2.

In the energy-minimized average conformation of the E318(6.30)R mutant, the side chain of Arg-173(3.50) had salt bridge/hydrogen bonding interactions with Asp-172(3.49). These interactions were not observed in the models of the wild type receptor. The side chain of Arg-318(6.30) had hydrogen bonding interactions with the backbone carbonyl moiety of Ala-176(3.53) and the backbone CO and side chain OH moieties of Ser-314(6.26) (Fig. 2*f*).

In the energy-minimized average conformation of V328(6.40)A, the OE1 atom of the Glu-318(6.30) side chain had hydrogen bonding interactions with Arg-173(3.50) and Thr-109(2.39), whereas the OE2 atom of Glu-318(6.30) had hydrogen bonding interactions with Asn-317(6.29) and Lys-385(7.58) (Fig. 2*g*). Comparison of the highly constitutively active mutants V328(6.40)A and E318(6.30)R with the other constructs (models 2) revealed important differences in hydrogen bonding interactions in the polar pocket between helices 1, 2, and 7. The Asp-120(2.50) side chain attained conformations that allowed it to interact with the NH_2 moiety of both Asn-92(1.50) and Asn-376(3.49) in the models of V328(6.40)A and E318(6.30)R and with the NH_2 moiety of Asn-376(7.49) and the backbone moiety of Thr-88(1.46) and Ser-373(7.46) in the model of the double mutant (R173(3.50)E/E318(6.30)R).

Hydrophobic Type Interactions between Transmembrane Helices—It is possible that interhelical interactions between hydrophobic residues may also contribute to constraining the wild type receptor to its inactive state conformation. The side chains of three hydrophobic residues in H6 where alanine substitution induces activation formed strong Van der Waals interactions with residues in adjacent helices in model 1 (Cys-322(6.34): Arg-173(3.50), Ile-177(3.54), Tyr-254(5.58), and Ile-258(5.62); Val-324(6.36): Val-379(7.52), Phe-383(7.56), and Asn-384(7.57); Val-328(6.40): Leu-113(2.43), Leu-166(3.43), Asn-376(7.49), and Val-379(7.52)). Comparison of the different models obtained by energy minimization of the average over the last 500 ps in molecular dynamics trajectories (models 2) revealed that the surface exposure of the Val-324(6.36) side chain differed markedly (ratio of accessible surface of Val-324(6.36) relative to standard exposed surface for the residue type as follows: R173(3.50)E/E318(6.30)R: 0.06; WT: 0.23; V328(6.40)A: 0.27; E318(6.30)R: 0.49). In model 2 of the double mutant, the Val-324(6.36) side chain was buried among Lys-323(6.35), Leu-325(6.37), Val-379(7.52), Tyr-380(7.53), Asn-384(7.57), and Phe-383(7.56) close to the intracellular end of H6 and H7.

Mutation Analysis of Residues Predicted to Form a Strong Ionic Interaction—To test the prediction of the modeling studies that Arg-173 and Glu-318 formed a strong ionic interaction, R173(3.50)E and E318(6.30)R as well as a double mutant con-

FIG. 2. **Models of the wild type rat 5-HT_{2A} receptor (models 1 and 2), R173E/E318R double mutant (models 1 and 2), E318R (model 2), and V328A (model 2).** *Left column*, models 1 obtained by using computer graphics and molecular mechanics energy calculations and the x-ray structure of bovine rhodopsin as a template. *a* and *b*, the wild type 5-HT2A receptor viewed from the intracellular side in a view perpendicular to the membrane surface. Residues where mutation to alanine increased potency of 5-HT-stimulated PI hydrolysis (*red*, oxygen; *blue*, nitrogen; *white*, carbon; *yellow*, sulfur) and residues within a 3.0-Å radius of such residues in other helices (*orange*) are shown. *b*, residues where mutation to alanine decreased (*colored* by atom type) or had no effect on (*colored green*) potency of 5-HT-stimulated PI hydrolysis and Glu-318(6.30) (*colored orange*) are shown. *c*, a close up view of the intracellular parts of helices 3 and 6 in the wild type and R173(3.50)E/E318(6.30)R models 1 (the junction between the helices and the intracellular domains is at the *top* in the *figure*) showing hydrogen bonding interactions as *yellow lines*. *Right column* (*d–g*), models 2 obtained by energy minimization of an average over the last 500 ps in molecular dynamics trajectories showing the WT, double mutant (E318(6.30)R/R173(3.50)E), E318(6.30)R, and V328(6.40)A, respectively. The side chains of residues at positions 3.50 and 6.30 and residues having hydrogen bonding interactions (*yellow lines*) with these are displayed in *ball and stick* representations. *Blue*, Asp and Glu; *red*, Lys and Arg. Residues having hydrogen bonding interactions with residues at positions 3.50 and 6.30 are *color-coded* by atom type (*red*, oxygen; *blue*, nitrogen; *white*, carbon; *grey*, hydrogen). The mutated amino acid Ala-328 (6.48) and Val-375 (7.48) in H7 are displayed in CPK representation.

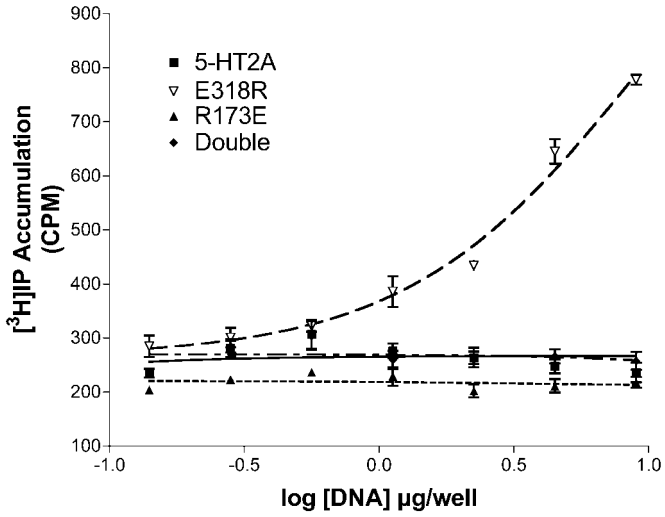

FIG. 3. **Basal PI hydrolysis of WT and mutant 5-HT2A receptors.** Values represent mean cpm of tritiated inositol ± S.E. collected from three separate experiments each with triplicate determinations. Data are plotted as a function of μg of receptor DNA used to transfect HEK 293 cells in six-well microtiter plates.

taining both mutations in a single plasmid were constructed. As shown in Table III, receptor expression of the mutant constructs was variable but consistently greater than 200 fmol/mg. Notably, the double mutant expressed functional receptor at ~618 fmol/mg, intermediate between R173(3.50)E and the WT receptor. The binding of [^{3}H]ketanserin was not significantly affected by any of the mutations. Agonist (5-HT) affinity, however, increased 10-fold in the E318(6.30)R mutant as predicted. Receptor activation, as measured by PI hydrolysis, was most severely inhibited by the R173(3.50)E mutation (Table III), which showed a 32-fold decrease in agonist potency. Conversely, the E318(6.30)R mutation produced a 23-fold decrease in potency. The double mutant E318(6.30)R/R173(3.50)E recovered some but not all of the WT phenotype, yielding an EC_{50} for 5-HT 12-fold higher than the unmutated 2A receptor.

Basal PI hydrolysis was also examined for each of the mutants used in this experiment. A titration of the cDNA used to transfect HEK cells was performed, and the basal (unstimulated) level of PI hydrolysis was measured (Fig. 3). Only the E318(6.50)R mutant produced a detectable concentration-dependent increase in basal PI hydrolysis (*i.e.* constitutive PI hydrolysis activity). Basal, agonist-independent PI hydrolysis increased with increasing DNA transfection concentration and was detectable to below 0.5 μg of DNA transfected per well of a six-well culture plate. Untransfected HEK 293 cells displayed less than 225 cpm (background) under the assay conditions used (data not shown).

R-SAT Assays Confirm PI Activation Data and Accurately Predict Constitutive Activity of Native and Mutant 5-HT2A Receptors—R-SAT assays were then used to further define the functional effects of the various 5-HT2A receptor mutants. Seven selected receptor constructs representing the interface between H3 and the i2 loop (R173(3.50)E), H6 (N317(6.29)A, E318A(6.30)A, E318(6.30)R, K320(6.32)A, and V328(6.40)A) and the double mutant (R173E/E318R) were chosen for R-SAT analysis, and their respective potencies for the full agonist serotonin, the full inverse agonist ritanserin, and their corresponding degrees of constitutive signaling were determined. A titration of the cDNAs used to transfect NIH3T3 cells as part of the R-SAT assay was performed. As depicted in Fig. 4*a*, each receptor mutant displayed a distinct and quantifiable degree of basal signaling, which increased in a DNA concentration-dependent manner. As depicted in Fig. 4 and Table IV, the WT 5-HT2A receptor displayed a moderate degree of basal signaling (18 ± 2%) in this assay. Mutagenesis of R173(3.50)E created a significantly impaired receptor characterized by a complete loss of basal signaling and a 60-fold decrease in potency for serotonin (Fig. 4*b* and Table IV). The opposite phenotype was observed for the E318(6.30)R mutant, which displayed profoundly enhanced biological activity. This receptor was nearly fully activated in the absence of 5-HT (89 ± 11% basal activity), precluding accurate determinations of functional potency for serotonin. Interestingly, this mutant receptor displayed a 6.4-fold *decrease* in functional potency for the inverse agonist ritanserin (Table IV). The double mutant R173(3.50)E/E318(6.30)R displayed an intermediate phenotype, with a functional potency for serotonin 7.6-fold greater than the R173(6.30)E mutant yet 9.3-fold less than wild type and a measurable but minimal degree of basal activity (3.8 ± 2%). As depicted in Fig. 4 and Table IV, the four remaining TM6 mutants displayed a range of constitutive activity phenotypes. The N317(6.29)A and K320(6.32)A mutants displayed a slight loss of function with 5.0- and 2.2-fold decreased potency for serotonin, respectively, coupled with a mild decrease in basal signaling. The E318(6.30)A and V328(6.40)A mutants displayed substantial and graded gain of function phenotypes characterized by increased potencies for serotonin (1.7- and 33-fold, respectively) and decreased potencies for ritanserin (1.5- and 9.5-fold, respectively). These receptor mutants displayed significant increases in basal signaling from the 18% seen with the wild type receptor to 45 and 76%, respectively. In summary, the rank order of constitutive activity of these 5HT2A receptors as measured in this assay was R173(3.50)E < R173E/E318R double mutant < N317(6.29)A = K320(6.32)A < WT ≪ E318(6.30)A ≪ V328(6.40)A = E318(6.30)R.

DISCUSSION

The main findings of this study are that 1) a strong ionic interaction (*i.e.* "salt bridge") between Arg-173(3.50) in H3 and Glu-318(6.30) in H6 of the 5-HT2A receptor stabilizes the inactive state of the receptor, 2) disruption of this interaction leads to constitutive activation of the 5-HT2A receptor, 3) hydrophobic interactions also appear to stabilize the inactive state of the 5-HT2A receptor, and 4) functional expression of directed H3 and H6 mutants that disrupt these normal interactions can affect receptor expression as well as dramatically affect potency for receptor agonists and inverse agonists.

In this study, we examined the effect of mutation of the residues in the N-terminal part of H6 on receptor activation in an attempt to determine the extent to which the residues in this region play a role in receptor activation. It has been previously suggested that residues in the third intracellular loop of the 5-HT2A receptor may be responsible for interactions with G-proteins (G_q) and the transmission of subsequent effector function (1), although direct tests of this hypothesis have not been made previously.

The data from Table II suggest that a number of residues in this region (Asn-317(6.29), Glu-318(6.30), Gln-319(6.31), Lys-320(6.32), Cys-322(6.34), Val-324(6.36), Leu-325(6.37), and Val-328(6.40)) all participate in the regulation of receptor activity. Our current working model hypothesizes that the receptor is stabilized in a "ground" or inactive state by interaction of a number of charged and noncharged residues. Our model also predicts that agonist binding is accompanied by a rotation of TM6, leading to a subsequent rotational movement of H6 and disruption of key stabilizing ionic interactions between residues of H6 and residues at the *i*2/H3 interface, although the current study does not provide biochemical confirmation of this prediction. Of the residues mutated in this study, those that decreased potency after mutation to alanine are all predicted to

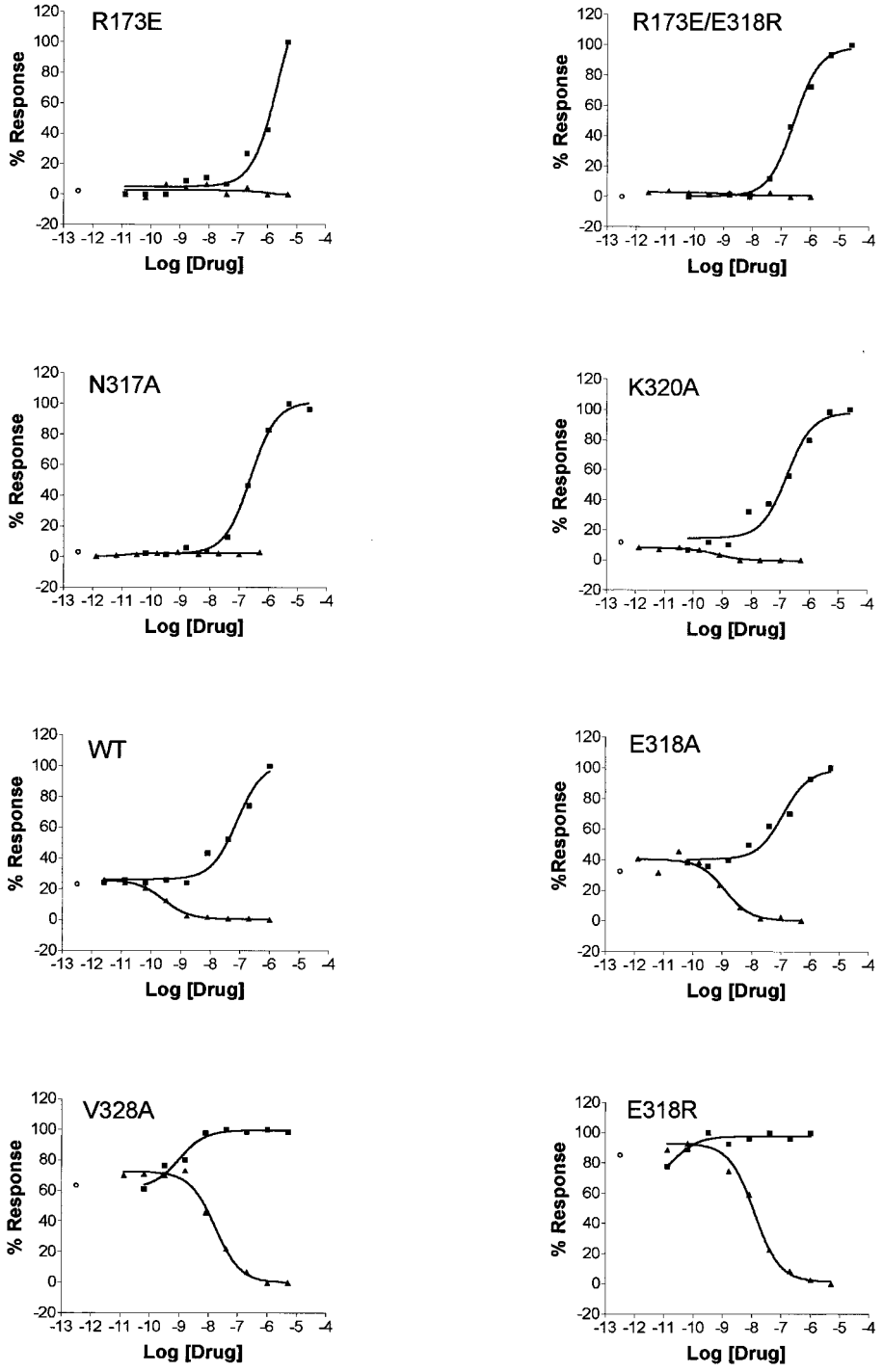

FIG. 4. **Constitutive activity of 5-HT2A receptor mutants revealed by R-SAT.** Reciprocal mutations of the H3 and H6 drastically affect 5HT2A receptor basal signaling properties. *a*, constitutive activity as a function of DNA concentration. NIH-3T3 cells were transiently transfected with 0.5–50 ng/well receptor DNA as part of the R-SAT assay. Constitutive activity was defined as (basal response — full inverse agonist response)/(full agonist response — full inverse agonist response) shown to reach maximal levels at ~25 ng/well receptor DNA. Data are derived from 3–5 separate experiments. S.E. bars have been omitted for clarity but were all less than 15%. *b*, representative concentration response curves are shown for the full agonist serotonin (*filled squares*) and the inverse agonist ritanserin (*filled diamonds*) for each of the receptor mutants assessed at 25 ng/well of plasmid DNA. Data are plotted as the percentage response observed in the R-SAT assay, defined as full agonist response/full inverse agonist response. The data are from nine-point concentration-response curves performed in duplicate. Control (no drug treatment) values are depicted on the *left* of each *graph*.

be involved in intra- and interhelical hydrogen bonding interactions. Such intra- and interhelical hydrogen bonding interactions might play an important structural role in stabilizing active state conformations. We cannot exclude the possibility that the N317(6.29)A, Q319(6.31)A, and K320(6.32)A mutations specifically disrupt hydrogen bonding interactions with the G_q protein. Studies in progress[2] predict that portions of the *i*3 loop may directly interact with $G\alpha_q$.

The (E/D)RY motif near the cytoplasmic end of TM3 is highly conserved among the seven-transmembrane GPCRs.[3] Within this motif, Arg-3.50 is almost fully conserved in family 1 GPCRs (Arg in 98% of the sequences in the tGRAP10 family 1 alignment). There is now a growing body of evidence suggesting that Arg-173(3.50) plays an important role in activation of several GPCRs (15, 21, 31–33), although without a defined mechanism. In support of our current hypothesis, and in direct agreement with our findings, R135(3.50)W and R135(3.50)L mutant rhodopsin receptors were found to be spectrally normal (each bound 11-cis-retinal and was converted to the alternate spectral form with λ_{max} = 380 nm upon illumination) but were defective in the signal transduction pathway (32). Related findings were reported for the α_{1B}-adrenergic receptor (31), in which D142(3.49)A caused significant constitutive activity. The effect of direct alanine mutation of Arg-3.50 on the activity of

[2] W. K. Kroeze and B. L. Roth, manuscript in preparation.
[3] A detailed alignment of GPCRs can be found on the World Wide Web at tGRAP.uit.no/fam1w.html.

TABLE IV
R-SAT reveals differences in constitutive activity among various 5-HT2A receptor mutants

Functional potencies for the full agonist serotonin and the full inverse agonist ritanserin as well as the constitutive activity for a series of receptor mutants are reported. All data are from R-SAT assays performed as detailed under "Materials and Methods." Data are from nine-point concentration response curves performed in duplicate. Potencies are reported as the average log EC_{50} ± S.D. from 3–10 separate experiments. Constitutive activity is defined as (basal response-full inverse agonist response)/(full agonist response-full inverse agonist response). ND, not detectable.

Construct	Log EC_{50} for 5-HT	Log EC_{50} for ritanserin	Constitutive activity
			%
WT	7.4 ± 0.2	9.5 ± 0.1	18 ± 2[a]
N317A	6.7 ± 0.3	ND	6.5 ± 2[a] (0.01)
E318A	7.6 ± 0.2	9.3 ± 0.2	45 ± 9[a] (0.01)
K320A	7.0 ± 0.3	ND	7.4 ± 2[a] (0.02)
V328A	ND	8.5 ± 0.2* (0.006)	76 ± 11[a] (0.01)
R173E	5.6 ± 0.2* (0.01)	ND	0[a]
E318R	ND	8.5 ± 0.2* (0.01)	89 ± 11[a] (0.02)
R173E/E318R	6.5 ± 0.1* (0.02)	ND	3.8 ± 2[a] (0.01)

[a] Significantly different from WT ($p \leq 0.05$).

the α_{1B}-adrenergic receptor was, however, undetermined. More convincingly, direct mutation of the homologous residue in gonadotropin-releasing hormone receptor to Gln, His, or Lys severely inhibited agonist-induced inositol phosphate generation (15). Finally, in a most recent analysis of homologous residues in the β_2-adrenergic receptor, the authors propose direct interaction of Arg-131(3.50) with Glu-268(6.30) and the neighboring Asp-130(3.49) (21). Together, these findings suggest an important role for Arg-173(3.50) in GPCR activation that appears to be conserved across all receptor families.

E318(6.30)A showed considerable constitutive receptor activity by R-SAT (45% of the maximum stimulatable activity), eclipsed only by V328(6.40)A (76%) and E318(6.30)R (89%). Both of the tested E318(6.30) mutants had 1) enhanced affinity for agonist binding, 2) enhanced potency for activation by 5-HT (as measured by PI hydrolysis and R-SAT), and 3) increased basal activity in both assay systems, all hallmarks of constitutive activity. Interestingly, only mutations in the 5HT2A receptor that induced profound constitutive activity (>70%, E318R and V328A) displayed decreased functional potencies for the full inverse agonist ritanserin. R-SAT confirmed the basal signaling properties of the mutant receptors and proved its utility for the measurement of inverse agonist responses in those receptors for which routine measurements of constitutive activity are unobtainable. The sensitivity of the R-SAT technology has already proven useful in identifying novel psychotherapeutic agents (*e.g.* antipsychotics) that differ more in their inverse agonist than antagonist properties (34).

Interestingly, the E318(6.30)R mutation elicited greater constitutive activity than E318(6.30)A, suggesting that a direct polar repulsion between this residue and Arg-173(3.50) is at least partially responsible for the constitutive phenotype. Results obtained with the E318(6.30)R mutant further suggest that, within the guidelines of allowable motion of H6, additional rotation of this segment away from the ground state conformation leads directly to increased receptor activity. The double (reciprocal) mutant E318(6.30)R/R173(3.50)E had a much reduced potency of 5-HT-stimulated PI hydrolysis and minimal constitutive activity (3%) compared with the wild type receptor. This could be explained by differences in the hydrogen bonding interactions observed between the WT and the reciprocal mutant during molecular dynamics simulations (Fig. 2, *d* and *e*) or after Monte Carlo simulations (Fig. 2*c*). During molecular dynamics simulations, stronger salt bridge/hydrogen bonding interactions between H3 and H6 were observed in the double mutant than in the wild type receptor. The Arg-318(6.30) side chain of the double mutant interacted with the Asp-172(3.49) and Glu-173(3.50) side chains (Fig. 2*e*), whereas the Arg-173(3.50) side chain of the wild type receptor interacted with Glu-318(6.30) (Fig. 2*d*). The R173(3.50)E mutant had also the characteristics of an inactive state conformation. Interhelical interactions between E3.50 and other residues may lock this mutant in the inactive state.

According to the present mutagenesis and modeling data, it is likely that interactions between hydrophobic residues in helix 6 (Cys-322(6.34), Val-324(6.36), Val-328(6.40)) and helices 5 and 7 also contribute to the stabilization of inactive state conformations. Amino acid substitutions at position 6.34 in rat 5-HT2A (35), rat 5-HT2C (36), and other family A receptors (*e.g.* Refs. 37–39) have been shown to lead to constitutive activity. Site-directed mutagenesis experiments with the G_q-coupled AT_{1A} angiotensin receptor have identified I245(6.40)L as one of 16 single point substitutions that induce constitutive activity (40). Finally, random saturation mutagenesis of TM6 in the muscarinic m5 receptor revealed a periodicity of mutants that induce constitutive receptor signaling, leading the authors to conclude that TM6 is involved in stabilizing the off state of the receptor and that rotational changes in this portion of the molecule were critical to receptor activation (18, 19, 25). Our systematic mutagenesis and modeling studies confirm that minor changes in the side chain volumes at the interfaces between helices 6 and 7 and between helices 6 and 5 promote constitutive receptor activation.

The molecular dynamics simulations of wild type and mutant receptors also suggested that the transition from inactive to active state conformations may involve a slight increase in distance between the intracellular halves of H6 and H7. Interestingly, the side chain of the highly conserved Asp-120(2.50) changed conformation in the simulations of the constitutively active mutants (V328(6.40)A and E318(6.30)R), leading to rearrangement in the hydrogen bonding interactions at the polar pocket between helices 1, 2, and 7. This observation supports previously incompletely explained findings from site-directed mutagenesis studies, which suggested that both the Asp-120 and Asn-376 side chains are essential for 5-HT2A receptor activation (7).

In conclusion, these studies imply that the ground (inactive) state of the 5-HT2A receptor is stabilized by both ionic and novel hydrophobic interactions involving residues in the intracellular half of H6. A strong ionic interaction between Glu-318(6.30) and Arg-173(3.50) was confirmed to be a major factor in stabilizing the ground state of the 5-HT2A receptor. Finally, R-SAT technology was used to precisely quantify the constitutive activity of native and mutant GPCRs, providing insight into the structural requirements for receptor activation.

Acknowledgment—We acknowledge the excellent technical assistance of Brady Moore (Acadia Pharmaceuticals).

REFERENCES

1. Roth, B. L., Willins, D. L., Kristiansen, K., and Kroeze, W. K. (1998) *Pharmacol. Ther.* **79,** 231–257
2. Roth, B. L., Lopez, E., Patel, S., and Kroeze, W. K. (2000) *Neuroscientist* **6,** 252–262
3. Roth, B. L., and Willins, D. L. (1999) *Neuron* **23,** 629–631
4. Bhatnagar, A., Willins, D. L., Gray, J. A., Woods, J., Benovic, J. L., and Roth, B. L. (2001) *J. Biol. Chem.* **276,** 8269–8277
5. Almaula, N., Ebersole, B. J., Zhang, D., Weinstein, H., and Sealfon, S. C. (1996) *J. Biol. Chem.* **271,** 14672–14675
6. Shapiro, D. A., Kristiansen, K., Kroeze, W. K., and Roth, B. L. (2000) *Mol. Pharmacol.* **58,** 877–886
7. Sealfon, S. C., Chi, L., Ebersole, B. J., Rodic, V., Zhang, D., Ballesteros, J. A., and Weinstein, H. (1995) *J. Biol. Chem.* **270,** 16683–16688
8. Choudhary, M. S., Craigo, S., and Roth, B. L. (1993) *Mol. Pharmacol.* **43,** 755–761
9. Kristiansen, K. R., Kroeze, W. K., Willins, D. L., Gelber, E. I., Savage, J. E.,

Glennon, R. A., and Roth, B. L. (2000) *J. Pharmacol. Exp. Ther.* **293,** 735–746
10. Wang, C. D., Gallaher, T. K., and Shih, J. C. (1993) *Mol. Pharmacol.* **43,** 931–940
11. Porter, J. E., and Perez, D. M. (1999) *J. Biol. Chem.* **274,** 34535–34538
12. Porter, J. E., Hwa, J., and Perez, D. M. (1996) *J. Biol. Chem.* **271,** 28318–28323
13. Robinson, P. R., Cohen, G. B., Zhukovsky, E. A., and Oprian, D. D. (1992) *Neuron* **9,** 719–725
14. Zhou, W., Flanagan, C., Ballesteros, J. A., Konvicka, K., Davidson, J. S., Weinstein, H., Millar, R. P., and Sealfon, S. C. (1993) *Mol. Pharmacol.* **45,** 165–170
15. Ballesteros, J. A., Kitanovic, S., Guarnieri, F., Davies, P., Fromme, B. J., Konvicka, K., Chi, L., Millar, R. P., Davidson, J. S., Weinstein, H., and Sealfon, S. C. (1998) *J. Biol. Chem.* **273,** 10445–10453
16. Gether, U., Lin, S., Ghanouni, P., Ballesteros, J. A., Weinstein, H., and Kobilka, B. K. (1997) *EMBO J.* **16,** 6737–6747
17. Kobilka, B. K., and Gether, U. (1998) *Adv. Pharmacol.* **42,** 470–473
18. Spalding, T. A., Burstein, E. S., Wells, J. W., and Brann, M. R. (1997) *Biochemistry* **36,** 10109–10116
19. Burstein, E. S., Spalding, T. A., and Brann, M. R. (1998) *J. Biol. Chem.* **273,** 24322–24327
20. Palczewski, K., Kumasaka, T., Hori, T., Behnke, C. A., Motoshima, H., Fox, B. A., Le Trong, I., Teller, D. C., Okada, T., Stenkamp, R. E., Yamamoto, M., and Miyano, M. (2000) *Science* **289,** 739–745
21. Ballesteros, J. A., Jensen, A. D., Liapakis, G., Rasmussen, S. G., Shi, L., Gether, U., and Javitch, J. A. (2001) *J. Biol. Chem.* **276,** 29171–29177
22. Roth, B. L., Shoham, M., Choudhary, M. S., and Khan, N. (1997) *Mol. Pharmacol.* **52,** 259–266
23. Ballesteros, J. A., and Weinstein, H. (1995) *Methods Neurosci.* **25,** 366–428
24. Price, R. D., Weiner, D. M., Chang, M. S. S., and Sanders-Bush, E. (2001) *J. Biol. Chem.* **276,** 44663–44668
25. Spalding, T. A., Burstein, E. S., Henderson, S. C., Ducote, K. R., and Brann, M. R. (1998) *J. Biol. Chem.* **273,** 21563–21568
26. Cornell, W. D., Ciaplak, P., Bayly, C. I., Gould, I. R., Merz, K. M. J., Ferguson, D. M., Spellmeyer, D. C., Fox, T., Caldwell, J. W., and Kollman, P. A. (1995) *J. Am. Chem. Soc.* **117,** 5179–5197
27. Abagyan, R., and Totrov, M. (1994) *J. Mol. Biol.* **235,** 983–1002
28. Vriend, G. (1990) *J. Mol. Graph.* **8,** 52–56
29. Guex, N., and Peitsch, M. C. (1997) *Electrophoresis* **18,** 2714–2723
30. Altenbach, C., Yang, K., Farrens, D. L., Farahbakhsh, Z. T., Khorana, H. G., and Hubbell, W. L. (1996) *Biochemistry* **35,** 12470–12478
31. Scheer, A., Fanelli, F., Costa, T., De Benedetti, P. G., and Cotecchia, S. (1996) *EMBO J.* **15,** 3566–3578
32. Min, K. C., Zvyaga, T. A., Cypess, A. M., and Sakmar, T. P. (1993) *J. Biol. Chem.* **268,** 9400–9404
33. Ohyama, K., Yamano, Y., Chaki, S., Kondo, T., and Inagami, T. (1992) *Biochem. Biophys. Res. Commun.* **189,** 677–683
34. Weiner, D. M., Burstein, E. S., Nash, N., Croston, G. E., Currier, E. A., Vanover, K. E., Harvey, S. C., Donohue, E., Hansen, H. C., Andersson, C. M., Spalding, T. A., Gibson, D. F., Krebs-Thomson, K., Powell, S. B., Geyer, M. A., Hacksell, U., and Brann, M. R. (2001) *J. Pharmacol. Exp. Ther.* **299,** 268–276
35. Egan, C. T., Herrick-Davis, K., and Teitler, M. (1998) *J. Pharmacol. Exp. Ther.* **286,** 85–90
36. Herrick-Davis, K., Egan, C., and Teitler, M. (1997) *J. Neurochem.* **69,** 1138–1144
37. Wurch, T., Colpaert, F. C., and Pauwels, P. J. (1999) *Br. J. Pharmacol.* **126,** 939–948
38. Lattion, A., Abuin, L., Nenniger-Tosato, M., and Cotecchia, S. (1999) *FEBS Lett.* **457,** 302–306
39. Pauwels, P. J., Gouble, A., and Wurch, T. (1999) *Biochem. J.* **343,** 435–442
40. Parnot, C., Bardin, S., Miserey-Lenkei, S., Guedin, D., Corvol, P., and Clauser, E. (2000) *Proc. Natl. Acad. Sci. U. S. A.* **97,** 7615–7620
41. B. L. Roth and D. A. Shapiro (2001) *Expert Opin. Ther. Targets* **5,** 685–695

THE JOURNAL OF BIOLOGICAL CHEMISTRY
Vol. 277, No. 20, Issue of May 17, p. 18244, 2002

Printed in U.S.A.

Additions and Corrections

Vol. 277 (2002) 11441–11449

Evidence for a model of agonist-induced activation of 5-hydroxytryptamine 2A serotonin receptors that involves the disruption of a strong ionic interaction between helices 3 and 6.

David A. Shapiro, Kurt Kristiansen, David M. Weiner, Wesley K. Kroeze, and Bryan L. Roth

Page 11446, first column, last paragraph: The last complete sentence, which states "As depicted in Fig. 4*a*, each receptor mutant displayed a distinct and quantifiable degree of basal signaling, which increased in a DNA concentration-dependent manner," should be deleted. While true, the statement refers to a figure that was not included in the final version. Similarly, the legend to Fig. 4 contains a reference to the same omitted figure (Fig. 4*a*). The legend to Fig. 4 contains the text appropriate for all graphics in Fig. 4. These changes do not affect the results or conclusions of the paper.